



**HAL**  
open science

# Investigation of Separation Efficiency Indicator for the Optimization of the Acetone–Methanol Extractive Distillation with Water.

Xinqiang You, Ivonne Rodríguez-Donis, Vincent Gerbaud

► **To cite this version:**

Xinqiang You, Ivonne Rodríguez-Donis, Vincent Gerbaud. Investigation of Separation Efficiency Indicator for the Optimization of the Acetone–Methanol Extractive Distillation with Water.. *Industrial and engineering chemistry research*, 2015, 54 (43), pp.10863-10875. 10.1021/acs.iecr.5b02015 . hal-03608027

**HAL Id: hal-03608027**

**<https://hal.science/hal-03608027>**

Submitted on 14 Mar 2022

**HAL** is a multi-disciplinary open access archive for the deposit and dissemination of scientific research documents, whether they are published or not. The documents may come from teaching and research institutions in France or abroad, or from public or private research centers.

L'archive ouverte pluridisciplinaire **HAL**, est destinée au dépôt et à la diffusion de documents scientifiques de niveau recherche, publiés ou non, émanant des établissements d'enseignement et de recherche français ou étrangers, des laboratoires publics ou privés.



## Open Archive TOULOUSE Archive Ouverte (OATAO)

OATAO is an open access repository that collects the work of Toulouse researchers and makes it freely available over the web where possible.

This is an author-deposited version published in : <http://oatao.univ-toulouse.fr/>  
Eprints ID : 15860

**To link to this article** : DOI : 10.1021/acs.iecr.5b02015  
URL : <http://pubs.acs.org/doi/abs/10.1021/acs.iecr.5b02015>

**To cite this version** : You, Xinqiang and Rodriguez-Donis, Ivonne and Gerbaud, Vincent *Investigation of Separation Efficiency Indicator for the Optimization of the Acetone–Methanol Extractive Distillation with Water*. (2015) *Industrial & Engineering Chemistry Research*, vol. 54 (n° 43). pp. 10863-10875. ISSN 0888-5885

Any correspondence concerning this service should be sent to the repository administrator: [staff-oatao@listes-diff.inp-toulouse.fr](mailto:staff-oatao@listes-diff.inp-toulouse.fr)

# Investigation of Separation Efficiency Indicator for the Optimization of the Acetone–Methanol Extractive Distillation with Water

Xinqiang You,<sup>†,‡</sup> Ivonne Rodriguez-Donis,<sup>†,‡</sup> and Vincent Gerbaud<sup>\*,†,‡</sup>

<sup>†</sup>Université de Toulouse, INP, UPS, LGC (Laboratoire de Génie Chimique), 4 allée Emile Monso, F-31432 Toulouse Cedex 04, France

<sup>‡</sup>CNRS, LGC (Laboratoire de Génie Chimique), F-31432 Toulouse Cedex 04, France

## Supporting Information

**ABSTRACT:** A multiobjective genetic algorithm optimization of the extractive distillation process of acetone–methanol minimum azeotropic mixture with heavy entrainer water is investigated. The process includes the extractive and entrainer regeneration columns, and the optimization minimizes the energy cost objective function (OF) and total annual cost (TAC) and maximizes efficiency indicators  $E_{\text{ext}}$  and  $e_{\text{ext}}$  that describe the ability of the extractive section to discriminate the product between the top and the bottom of that section. Earlier work (You et al. *Ind. Eng. Chem. Res.* **2015**, *54*, 491) found that improvement of some designs in the literature led to an increase in those indicators. A two-step optimization strategy for extractive distillation is conducted to find suitable values of the entrainer feed flow rate, entrainer and azeotropic mixture feed locations, total number of trays, two reflux ratios, and two distillates in both the extractive column and the entrainer regeneration column. The first step relies upon the use of a nonsorted genetic algorithm (NSGA) with the four aforementioned criteria. Second, the best design taken from the GA Pareto front is further optimized focusing on decreasing the energy cost by using a sequential quadratic programming (SQP) method. In this way, the most suitable design with optimal efficiency indicators, low energy consumption, and low cost are obtained. Analyzed with respect to thermodynamic insights underlying the extractive section composition profile map, the Pareto front results show that there is maximum  $E_{\text{ext}}$  at a given reflux ratio, and there is minimum reflux ratio for a given  $E_{\text{ext}}$ . There is an optimal efficiency indicator  $E_{\text{ext,opt}}$  which corresponds to the minimum TAC taken as the best design. In other words,  $E_{\text{ext,opt}}$  can be a criterion for the comparison between different designs for the same separating system. A SQP-based design is only <1% better in TAC than the best NSGA design, showing that this later method is able to find a consistent design for the extractive process concerning the 1.0-1a class mixture.

## 1. INTRODUCTION

Extractive distillation is commonly applied in industry for separating azeotropic or low relative volatility liquid mixtures by adding an entrainer and is becoming a more and more important separation method in petrochemical engineering because of the energy and capital cost savings.<sup>1,2</sup> A suitable entrainer should interact preferably with one of the components of the original mixture and alters their relative volatilities.<sup>3</sup> The main distinction between extractive distillation and azeotropic distillation is that the entrainer is fed at a different location than the main mixture, bringing an additional extractive section in the column between the usual stripping and/or the rectifying sections.<sup>4</sup>

Extractive distillation can be operated in both batch and continuous modes. Batch mode has the advantage in operating flexibility, and continuous mode has the advantage in large-scale production.<sup>5–7</sup> In this work, the configuration of continuous extractive distillation enabling a direct split suitable for the minimum boiling azeotrope mixture separation with a heavy entrainer (class 1.0-1a)<sup>4</sup> is used. As shown in Figure 1, the entrainer is fed between the top tray and the main feed, giving rise to rectifying, extractive, and stripping sections in the extractive column. For A–B minimum azeotrope mixture (boiling temperature of A is lower than that of B) with entrainer E, A (B) is the distillate of the extractive distillation column when the univolatility line reaches the AE (BE) side.

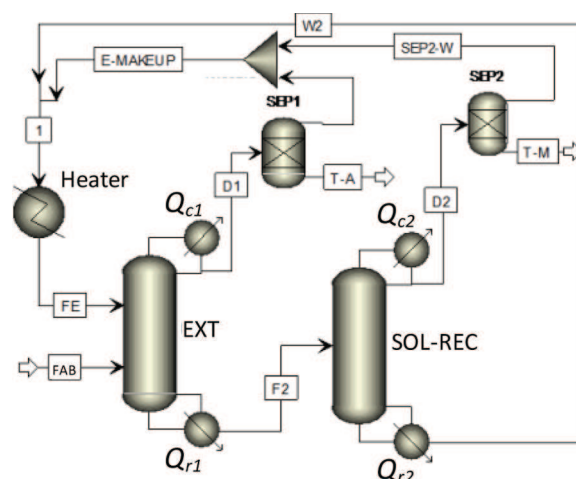


Figure 1. Extractive distillation flow sheet.

The mixture of E with the nonproduct component in extractive distillation B (A) is fed to the entrainer regeneration column

where B (A) is removed as distillate, and E is recovered as bottom product. The entrainer is cooled and recycled to the extractive column with some entrainer makeup due to the entrainer loss in the two distillate streams. The process needs a makeup entrainer to compensate its losses with the products. As the flow rate of makeup entrainer is not known beforehand, we set it equal to the entrainer losses combined after sharp splits by using SEP1 and SEP2 on the two product distillates. Although SEP1 and SEP2 are virtual, the flow sheet can represent the real flow sheet of the extractive distillation in closed mode.

Nowadays, the hot topics in extractive distillation are entrainer selection and process design and optimization. A thorough knowledge of the thermodynamic properties of the mixtures not only is useful for the entrainer selection and process design but also can explain optimization results, as we shall show in this paper. The choice of a suitable entrainer affects the feasibility and efficiency of extractive distillation processes. Residue curve maps have been proven to be a very useful topological tool for the analysis of the thermodynamic behavior of ternary azeotropic mixtures.<sup>8,9</sup> Ravagnani et al.<sup>10</sup> compared ethylene glycol and tetra-ethylene glycol as entrainer for anhydrous ethanol production and used the residue curve maps tool to analyze the proposed processes in interpreting the mixture behaviors and feasibility of the distillation column. But in the general case, the position of the univolatility line in the residue curve map sets the volatility order region and defines the product to be withdrawn.<sup>11–14</sup> Alternatively, inflection point curves can be used.<sup>15</sup> In addition, it also hints at the occurrence of a limiting entrainer-to-feed flow rate ratio value for the separation to be effective. A general feasibility criterion for homogeneous batch extractive distillation under infinite reflux ratio was proposed by Rodriguez-Donis et al.<sup>11</sup> based on the analysis of the residue curve map and the univolatility line. Process feasibility under finite reflux was also described in these articles. For a continuous process, the feasibility criterion holds but there exists a minimum bound for the entrainer flow rate ratio and minimum and maximum bounds for the reflux ratio for the process to be feasible, as was reported previously.<sup>15–17</sup>

On the other hand, there are many contributions in the literature focusing on extractive distillation process design and optimization. Compared with a simple conventional distillation, the difficulties of the extractive distillation process design lie in a greater number of degrees of freedom and the recommended recycling of the entrainer with as little impurity as possible. The entrainer choice, entrainer flow rate, and entrainer feed location are the additional degrees of freedom. The optimization of extractive distillation is usually considered as a large size problem because of the solving of a significant number of strongly nonlinear equations. In addition, suitable initial values are needed for solving the nonlinear programming (NLP) subproblems and avoiding nonconvergence of the simulations.<sup>18</sup> When integer variables like feed locations and tray numbers are considered, the problem becomes a mixed-integer nonlinear programming (MINLP) problem. For the finding of the most suitable design of the extractive distillation, various techniques can be used, such as sensitivity analysis,<sup>19,20</sup> sequential iterative optimization,<sup>21</sup> and various optimization methods such as sequential quadratic programming (SQP) for NLP problems,<sup>22,23</sup> mixed-integer nonlinear programming (MINLP),<sup>24,25</sup> genetic algorithm (GA)<sup>26,27</sup> for MINLP problems, and so on.

In our previous work, we intended to assess the engineering and physical meaning of an optimal extractive distillation design based on the knowledge of thermodynamic insights from the residue curve map and univolatility line for extractive distillation. We ran the optimization of the acetone–methanol minimum azeotropic mixture extractive distillation with water as heavy entrainer by using a two-step optimization procedure.<sup>28</sup> The optimization process led to double-digit savings in energy consumption and total annual cost (TAC) compared to literature values. The lower pressure in the extractive column was deduced from thermodynamic insight analysis and proved to be beneficial. For comparing with the design in literature, we fixed the total number of trays as proposed in Luyben's design.<sup>2,19</sup> We then defined two indicators, the total extractive efficiency and the extractive efficiency per tray, which describe the ability of the extractive section to discriminate the product between the top and bottom of that section. We then showed with these indicators that the design in the literature could be improved by increasing the efficiency indicators.

In this study, we investigate whether an optimal extractive distillation design corresponds to maximum values of those efficiency indicators and why this is not the case by combining optimization techniques with analysis of thermodynamic insights underlying the extractive section composition profile map. We go a step further than in our previous work by relaxing the constraints on the total number of trays and by considering the efficiency indicators  $E_{\text{ext}}$  and  $e_{\text{ext}}$  as optimization criterions. A multiobjective genetic algorithm is connected through Excel with Aspen Simulator to minimize energy cost and TAC and maximize  $E_{\text{ext}}$  and  $e_{\text{ext}}$ . The minimum boiling azeotropic mixture acetone–methanol with water as entrainer (class 1.0-1a) is taken as an example of the optimization process. As the most-studied mixture, it allows us to compare the extractive distillation process designs with each other.

## 2. BACKGROUND, METHOD, AND OBJECTIVE FUNCTION

### 2.1. Topological Features of Class 1.0-1a Extractive Distillation Process.

A feasible design should connect the extractive section with the rectifying section (in batch and continuous modes) and with the stripping section (in continuous mode).<sup>16</sup> The general feasibility criterion enounced by Rodriguez-Donis and co-workers<sup>4,11,14</sup> and originated from former studies<sup>1,3,8,12,13</sup> strictly holds for infinite reflux operation for batch process because in continuous process there is always a maximum feasible finite reflux ratio.<sup>14–17</sup> Indeed, for finite reflux, things are more complicated and can only be exhaustively studied from the knowledge of the pinch point trajectories under the assumption of infinite number of trays and more generally of the extractive singular point locations under finite number of trays.<sup>15–17,29–31</sup> Graphical,<sup>15,16</sup> shortcut,<sup>17–30</sup> and numerical<sup>29,31</sup> methods were proposed. Those works showed that the key factor lies in the extractive section ability to intersect the rectifying section and that feasible and unfeasible regions could be found and are related to minimum and maximum values of the reflux ratio and of the entrainer feed flow rate. The general criterion devised for batch operation under infinite reflux ratio<sup>11</sup> can hold for continuous operation under finite reflux ratio.<sup>14</sup> For continuous extractive distillation, minimum entrainer flow rate and minimum energy limit exist and require an infinite number of stages to obtain desired product purities and a very large entrainer flow rate for the

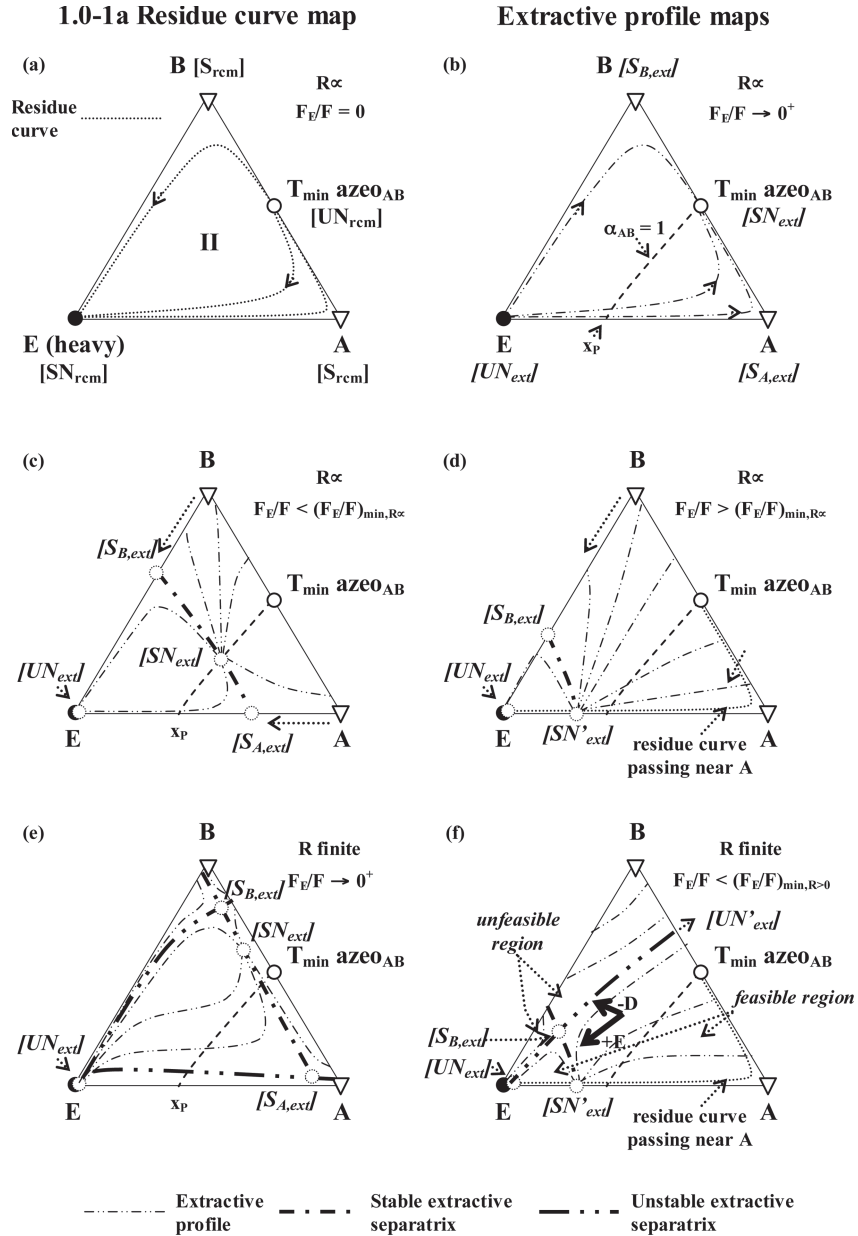


**Figure 2.** Topological features of class 1.0-1a with heavy entrainer in extractive distillation process operation (adapted from Rodriguez-Donis et al.<sup>11</sup>).

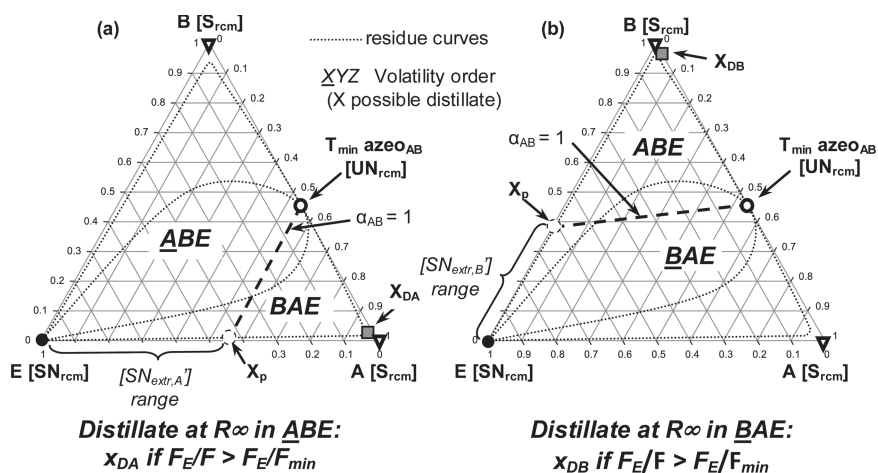
minimum energy case.<sup>14,15</sup> A maximum reflux ratio limit also exists to “connect” all three sections’ composition profiles.<sup>16,17,30,31</sup> Shen et al.<sup>14</sup> noted that the feasible parameter range for reflux ratio and entrainer-to-feed flow rate ratio is smaller for continuous operation because of the additional requirement of connecting the stripping and the extractive profile.

Figure 2 displays the qualitative topological features of the class 1.0-1a diagram extractive section composition profile map originally analyzed for the batch extractive process because it will be used in Results and Discussion.

Feasible and unfeasible regions for the composition in the extractive section of the column are deduced from the analysis of the extractive composition profile map, similarly to residue curve map (RCM) analysis. The feasible composition regions will encompass the extractive section composition profile in the extractive distillation column obtained as results. Those regions

are bounded by extractive stable and unstable separatrices which connect stable and unstable nodes, respectively, to saddle points and cross at saddle extractive singular points.<sup>31,32</sup> For the class 1.0-1a, the pinch point of the extractive composition profiles is a stable extractive node  $SN_{ext}$  issued from the original minimum boiling azeotrope. Saddle extractive points,  $S_{i,ext}$ , emerge from the RCM saddle points (A and B vertices). An extractive unstable node,  $UN_{ext}$ , is located near the entrainer vertex.

At infinite reflux which concerns only the batch extractive process, while  $F_E/F$  increases (Figure 2c),  $SN_{ext}$  moves along  $\alpha_{AB} = 1$ ,  $S_{A,ext}$  and  $S_{B,ext}$  move along the binary edges (A-E and B-E, respectively), toward the vertex (E), which is the entrainer. Extractive stable separatrices that link  $SN_{ext} - S_{A,ext} - S_{B,ext}$  move inside the composition triangle toward E with no effect on feasibility because of infinite reflux ratio.



**Figure 3.** Thermodynamic features of 1.0-1a mixtures. Separation of a minimum boiling azeotrope with a heavy entrainer (adapted from Shen et al.<sup>14</sup>).

Close to a limiting value  $F_E/F_{\min,R\infty}$   $SN_{\text{ext}}$  and  $S_{A,\text{ext}}$  merge and the extractive composition profiles are attracted to a new extractive stable node,  $SN_{\text{ext}}'$ , located below the A-E edge.  $F_E/F_{\min,R\infty}$  is defined as the value for which the process becomes feasible: Extractive composition profiles ending at  $SN_{\text{ext}}'$  cross a rectifying profile that can reach the vicinity of the expected product (A) (see Figure 2d).

At finite reflux as  $F_E/F$  increases, the extractive unstable separatrix  $UN_{\text{ext}}-S_{A,\text{ext}}-UN_{\text{ext}}'$  near the A-E edge holds (see Figure 2e) until  $SN_{\text{ext}}$  and  $S_{A,\text{ext}}$  merge at  $F_E/F_{\min,R>0} > F_E/F_{\min,R\infty}$  giving rise to  $SN_{\text{ext}}'$  (Figure 2f). In the meantime (Figure 2f),  $S_{B,\text{ext}}$  moves toward the vertex E inside the triangle. Consequently, the extractive unstable separatrix  $UN_{\text{ext}}-S_{B,\text{ext}}-UN_{\text{ext}}'$  remains and now sets unfeasible composition regions located above it (see Figure 2f) that prevent the total recovery of component A from the column. Knowledge of this unstable separatrix location will help us in the analysis of the optimization results. In addition, the extractive stable separatrix also remains, joining  $S_{B,\text{ext}}$  to  $SN_{\text{ext}}'$  and  $SN_{\text{ext}}''$  located outside the ternary composition space through the B-E edge. Notice that there exists a minimum reflux ratio  $R_{\min}$  at a given  $F_E/F$ . When  $R < R_{\min}$ , there is no feasible region for the extractive section profile. The size of the unfeasible region increases as  $R_{\min}$  decreases.

Therefore, finite reflux operation which concerns both the batch and continuous extractive process is feasible if  $F_E/F > F_E/F_{\min,R>0}$  and  $R > R_{\min}$ . Now, the more component E is fed to the column, the closer is  $SN_{\text{ext}}'$  to component E and away from the distillate that is close to component A (see Figure 2f). For a proper extractive distillation design, it is necessary to enable the extractive section composition at the entrainer feed tray location to reach  $SN_{\text{ext}}'$ . It allows the connection with a rectifying section that can reach a high-purity distillate near A, following approximately a residue curve shape.

**2.2. Product and Limiting Operating Parameter for Class 1.0-1a Extractive Distillation.** Figure 3 displays the essential features of the 1.0-1a class, corresponding to the separation of a minimum boiling azeotropic mixture A-B with a heavy entrainer E. The univolatility curve  $\alpha_{AB} = 1$  and the residue curve map features are also shown.

The Serafimov's class 1.0-1a occurrence in literature amounts to 21.6%.<sup>33</sup> With a heavy entrainer, the light original component A and the heavy original component B are both

residue curve map saddle points and form a minimum boiling azeotrope  $T_{\min} \text{ azeo}_{AB}$ , which is a RCM unstable node. The heavy entrainer E is a RCM stable node. The univolatility curve  $\alpha_{AB} = 1$  switches the volatility order of its concerned compounds, and volatility orders are ABE or BAE (see Figure 3) depending on the side.<sup>32</sup> In Figure 3a (3b), the  $\alpha_{AB} = 1$  curve intersects the binary side A-E (B-E) at the so-called point  $x_p$ . Then, A (B) is the expected product in the distillate because it is the most volatile in the region where it is connected to E by a residue curve of decreasing temperature from E to A (B). This matches the general feasibility criterion under infinite reflux ratio for extractive distillation.<sup>11</sup> The point  $x_p$  will give us information about the minimum content of entrainer ( $F_E/(F + F_E)$ ).<sup>28</sup> Below this value, the terminal point of the extractive section profiles,  $SN_{\text{ext}}'$ , lies on the univolatility curve. Above this value,  $SN_{\text{ext}}'$  leaves the univolatility curve to lie near the  $[x_p; E]$  segment.<sup>11,14</sup> Then the extractive profile can cross a rectifying profile, which is approximated by a residue curve under infinite reflux ratio and which reaches the vicinity of the product, ex. A (respectively B).

**2.3. Nonsorted Genetic Algorithm Process Optimization Technique.** Compared with other methods mentioned in the Introduction, the genetic algorithms are attractive in solving optimization problems with modular process simulators because of the following characteristics. Any simulator may fail to converge if unsuitable initial input values are set. When coupled with stochastic optimization techniques, this issue is less important as the search for optimal solution in genetic algorithm is not limited to one point but rather relies on several points simultaneously which build the population.<sup>34</sup> Second, in nonsorted genetic algorithm (NSGA), it is not necessary to have explicit information on the mathematical model or its derivatives because the algorithms are based on a direct search method. NSGA has been implemented in Excel with visual basic for applications (VBA) programming by our colleagues;<sup>34</sup> the result is the genetic algorithm library MULTIGEN. It can handle multiobjective constrained optimization problems involving mixed variables (boolean, integer, real), and some of these problems can be related to process structural optimization. Constraints as well as Pareto domination principles can be handled by the algorithms. Nonsorted genetic algorithm II (NSGAI) is the method we used. NSGAI is based on a ranking procedure, where the rank of each solution

is defined as the rank of the Pareto front to which it belongs. The diversity of nondominated solutions is guaranteed by using a crowding distance measurement, which is an estimation of the size of the largest cuboids enclosing a given solution without including any other. This crowding sorting avoids the use of the sharing parameter used in the previous version of the NSGA algorithm.<sup>34</sup>

The stable link between Excel and Aspen Plus was coded in VBA, as was done by Vazquez-Ojeda et al.<sup>18</sup> The node of variables such as tray number of column, reflux ratio, and so on are found by Aspen plus tools named *variable explorer*. The simulation is run by using the MESH model *Radfrac* in Aspen Plus.

**2.4. Advantages of NSGA for the Design of Extractive Distillation Process Compared with SQP.** Compared with the SQP optimization solver used in a previous work, NSGA brings several advantages, but may take much longer to perform successfully. First, because we usually choose a large population and may attempt to replace in the initial population nonconverging simulation by other parameters, the choice of the initial parameter values is less an issue. Second, we no longer have to choose two important aspects in extractive distillation: the choice of distillate flow rates, and the choice of open loop or closed-loop flow sheet. (1) Earlier, we chose the two distillate flow rates by sensitivity analysis<sup>28,35</sup> because their effects on the achievable product purity are strongly nonlinear. (2) The open loop flow sheet does not connect the recycled entrainer and the fresh entrainer feed. However, the closed-loop flow sheet (Figure 1) can be directly used in NSGA, and the effect of impurity in the recycled entrainer on the product purity is readily handled.

**2.5. Objective Function.** As in our previous study,<sup>28</sup> we minimize the total process energy consumption by introducing the objective function, OF. The differences in reboiler and condenser and the product prices are taken into account by using the energy price index ( $m$ ) and product price index ( $k$ ).

$$\min \text{OF} = \frac{Q_{r1} + m \cdot Q_{c1} + Q_{r2} + m \cdot Q_{c2}}{k \cdot D_1 + D_2}$$

subject to:  $x_{\text{acetone},D1} \geq 0.995$

$$x_{\text{methanol},D2} \geq 0.995 \quad (1)$$

With the use of the OF, the two columns in the extractive distillation process are evaluated simultaneously. Only the two product purities are regarded as constraints, and not the recycling entrainer purity, because of the use of NSGA in the closed-loop flow sheet.

The TAC is used as the second objective function for the comparison of the different designs. TAC includes capital cost per year and operating costs and is computed from the following formula:

$$\text{TAC} = \frac{\text{capital cost}}{\text{payback period}} + \text{operating cost} \quad (2)$$

The payback period is considered to be 3 years, and Douglas's cost formulas<sup>36</sup> are used with Marshall and Swift (M&S) inflation 2011 index<sup>37</sup> equal to 1518.1, for the sake of comparison with our previous work.<sup>28,35</sup> The capital cost includes the column shell cost, tray cost, and heat exchanger cost. The operating cost means the energy cost in the reboiler and condenser. To emphasize the effect of the entrainer flow

rate recycle on the process, the heat exchanger annual cost (heater in Figure 1) is taken into account. Other costs such as pumps, pipes, and valves are neglected at the conceptual design stage that we consider.

The efficiency indicator of extractive section  $E_{\text{ext}}$  and the efficiency indicator per tray in extractive section  $e_{\text{ext}}$  are the third and fourth objective function as  $E_{\text{ext}}$  and  $e_{\text{ext}}$  describe the ability of the extractive section to discriminate the desired product between the top and the bottom of the extractive section. The definition of the efficiency indicator for the extractive section is

$$E_{\text{ext}} = x_{p,H} - x_{p,L} \quad (3)$$

where  $E_{\text{ext}}$  is the total efficiency of the extractive section,  $x_{p,H}$  the product mole fraction at one end of the extractive section, and  $x_{p,L}$  the product mole fraction at another end of the extractive section. Here, we use the entrainer feed and the main feed tray locations as ends of the extractive section.

The definition of the efficiency indicator per tray in the extractive section is

$$e_{\text{ext}} = \frac{E_{\text{ext}}}{N_{\text{ext}}} \quad (4)$$

where  $e_{\text{ext}}$  is the efficiency indicator per tray and  $N_{\text{ext}}$  is the tray number of the extractive section. The efficiency indicator per tray  $e_{\text{ext}}$  is supplementary to  $E_{\text{ext}}$  for handling the different designs with different entrainer-to-feed flow rate ratios, different reflux ratios, and different tray numbers in the extractive section.

The vapor–liquid equilibrium (VLE) of the system acetone–methanol with water is described with the UNIQUAC thermodynamic model with the Aspen Plus built-in binary parameters<sup>28</sup> while the ideal vapor phase is assumed. The reliability of the VLE model has been assessed by Botia et al.<sup>38</sup> using vapor–liquid equilibrium experimental data under atmospheric and vacuum pressure. Notice that the tray number is counted from top to bottom of the column, and the condenser is considered as the first tray.

### 3. RESULTS AND DISCUSSION

**3.1. Problem Setting.** This work uses the extractive section efficiency indicator  $E_{\text{ext}}$  and  $e_{\text{ext}}$  for the first time as objective functions for the optimization of extractive distillation process, along with OF and TAC. Notice that energy cost OF and total annual cost are minimized, while the efficiency indicator for extractive section  $E_{\text{ext}}$  and per tray  $e_{\text{ext}}$  are maximized. Properly designed extractive distillation processes should have a low energy cost and TAC. These are related but are different in meaning. Typically, TAC depends on the cost method. It can vary depending on the different situations and it is used as a decision factor. Energy cost is connected to the process flow rate and mixture thermodynamics, and for the same thermodynamic model and same process design it will not vary. It is also useful for comparison when considering heat integrated processes. The maximization of both efficiency indicators, total  $E_{\text{ext}}$  and per tray  $e_{\text{ext}}$ , are duplicate in meaning but must be considered together for the following reason: removing the indicator per tray may lead to designs with unreasonably large tray numbers in the extractive section. That would correspond to large total efficiency indicator, large TAC, but probably minimum reflux operation and thus low energy cost OF.

For selecting the parameters of the GA, the tuning process is performed: several tests are conducted with different values of individual, crossover, and mutation fraction. After tuning, and owing to the fact that parameter ranges were not accurately determined as they could be with methods available in the literature<sup>15–18</sup> but defined over a wide range that encompassed values based on published extractive distillation design for the acetone–methanol–water system, we choose a large number of 300 individuals per generation. Other GA parameters were 0.8 for crossover fraction and 0.1 for mutation fraction. The NSGA optimization is stopped when the TAC cannot be reduced for 20 successive generations. The total number of generations are 270 in this study.

The procedure of the NSGA II method works as follows: First, the variables of the initial populations are generated randomly within the given value range in Excel (see ranges below). The variables of each individual are sent one by one to Aspen Plus software to run the simulation that gives back the product purities and other information for calculating objectives to Excel. Generally speaking, no feasible design that satisfies the constraints (product purities) is obtained in the first generation, but improvements come after some generations. For some meaningless designs identified with in-house VBA programming, for example no extractive section exists or the number of feed location is greater than the number of column stage, the product purities are set directly to zero without sending to Aspen. For the case that Aspen simulation is not converged or in error, the individual (design) will be discarded with the help of the Aspen run state parameter. For the extreme situation that all the individuals in the first generation are not converged or in error, NSGA will regenerate the first generation randomly. Second, based on the number of satisfied constraints, the population is divided into subpopulations. In our case, the better individuals are those that satisfy the two constraints (two product purities), then those that satisfy only one product purities, and then those that satisfy no product purities. The individuals in the subpopulation are ranked according to fitness function. Thanks to the different subpopulation, the GA can optimize the four objective functions and meanwhile minimizes the difference between the required and obtained product purities. Finally, the Pareto front is obtained as the results of the optimization of the extractive distillation process: a set of nondominated, optimal designs that satisfy the specification of the product purities. A design reported in the Pareto front means that it cannot be improved through one objective function without worsening the other objectives.

To compare with Luyben's work, the main feed flow rate is 540 kmol/h (equimolar acetone versus methanol) at 320 K, although we did find other optimal values in our previous work.<sup>28</sup> The 10 variables of the processes are tray number of the two column ( $N_1$  and  $N_2$ ); distillates and reflux ratios of the two column ( $D_1$ ,  $D_2$  and  $R_1$ ,  $R_2$ ), the feed locations of entrainer, main feed, and regeneration column ( $N_{FE}$ ,  $N_{FAB}$ ,  $N_{FR}$ ); and the entrainer flow rate  $F_E$  (which reflects  $F_E/F$ ). The value ranges are [10,100] for  $N_1$  and  $N_2$ ; [270.0, 271.3] for  $D_1$  and  $D_2$  (based on product recovery and purity); [0.1, 10] for  $R_1$  and  $R_2$ ; and [10,100] for  $N_{FE}$ ,  $N_{FAB}$ , and  $N_{FR}$  (some invalid situations such as  $N_{FE} \geq N_{FAB}$ ,  $N_{FAB} \geq N_1$ , and  $N_{FR} \geq N_1$  are excluded by VBA programming). Notice that the operating pressures of extractive column and entrainer generation column are set at 0.6 and 1 atm. We showed that a 0.6 atm leads to a lower  $(F_E/F)_{\min}$  and enhances the relative volatility between A

and B in the presence of E.<sup>28</sup> The pressure drop per tray was assumed to be 0.005 atm, and the tray efficiency is 85%.<sup>39</sup>

**3.2. Pareto Front of the Optimal Design Solution.** Although four objectives are used, the optimal design that we select is the one with the minimum TAC. The energy cost OF decreases with the increase of the column tray number, and it is useful for finding the minimum energy cost of each design. Regarding  $e_{\text{ext}}$  it is used to avoid the situation that only maximizing  $E_{\text{ext}}$  will result in too many trays used in the extractive section. Results of the stochastic optimization are displayed as approximate Pareto fronts in Figures 4–6. Figure 4

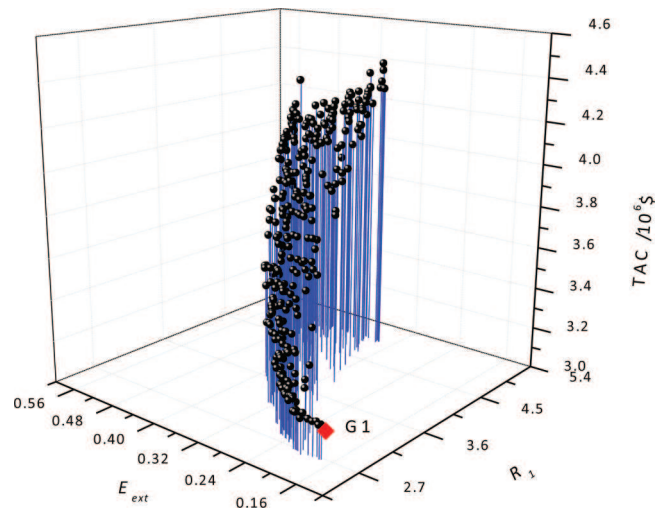


**Figure 4.** Approximate Pareto front of extractive distillation design for acetone–methanol–water system, TAC versus  $E_{\text{ext}}$  and  $R_1$ . The red diamond indicates G1.

shows the Pareto front of the acetone–methanol–water system, TAC versus  $E_{\text{ext}}$  and  $R_1$ . Figure 5 shows the Pareto front of TAC versus  $R_1$  and  $F_E$ , and Figure 6 shows the Pareto front of TAC versus  $e_{\text{ext}}$  and  $E_{\text{ext}}$ . The lowest TAC design is shown as G1 in Figures 4–6. Notice that for all 300 designs in the Pareto front, the target product purities and the recovery are satisfied. The recycling entrainer purity is not a constraint

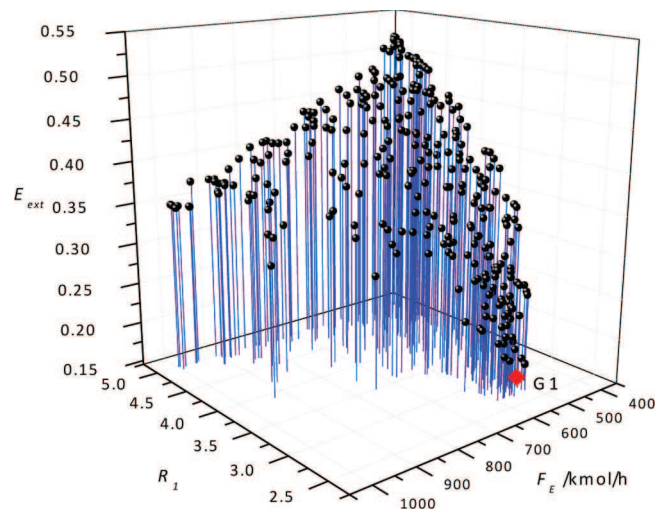


**Figure 5.** Approximate Pareto front of extractive distillation design for acetone–methanol–water system,  $E_{\text{ext}}$  versus  $R_1$  and  $F_E$ . The red diamond indicates G1.

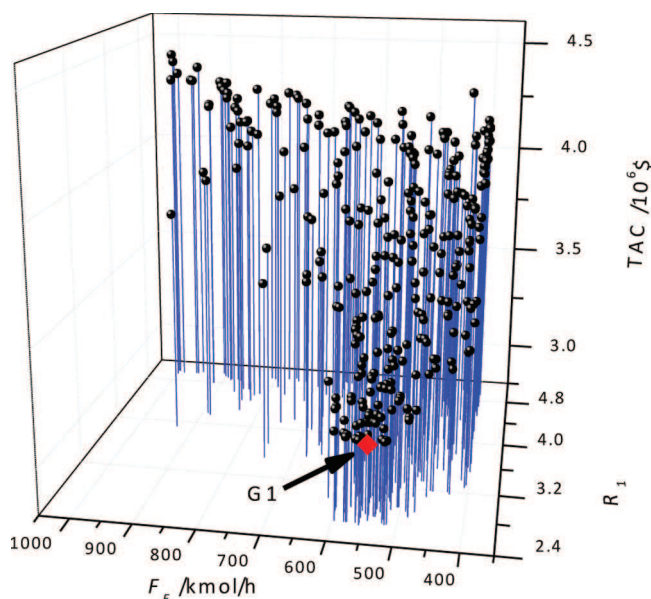


**Figure 6.** Approximate Pareto front of extractive distillation design for acetone–methanol–water system, TAC versus  $R_1$  and  $F_E$ . The red diamond indicates G1.

for the optimization process but remains very high, as will be seen later.

From Figure 4, we know the following: (1) The optimal design is not the one with maximum  $E_{\text{ext}}$ . Along with the decrease of  $E_{\text{ext}}$  and  $R_1$ , TAC decreases. Evidently, a low  $R_1$  is related to a low heat duty, and the operating cost and the TAC decreases. (2) For  $E_{\text{ext}}$ , this is not as straightforward. In other words,  $E_{\text{ext}}$  that we have thought to be maximized cannot be the unique criterion for optimizing the process. (3) The shape of the front shows that there is a maximum  $E_{\text{ext}}$  for a given reflux ratio, and there is a minimum  $R_1$  for a given  $E_{\text{ext}}$ . (4) Following the decrease of  $R_1$ , the value of  $E_{\text{ext}}$  decreases, and meanwhile, the value range of  $E_{\text{ext}}$  gets narrower. We can infer that a suitable design should correspond to an optimal efficiency  $E_{\text{ext,opt}}$  for which the minimum reflux ratio  $R_1$  exists.

From Figure 5, we know that (1) the highest efficiency indicator is located at highest reflux ratio and lowest entrainer flow rate. (2) The efficiency indicator increases at fixed reflux ratio while following the decrease of  $F_E$ . Recall from Figure 2 that  $R_1$  and  $F_E$  impact the unstable separatrix and that the stable node of extractive section  $\text{SN}_{\text{ext,A}'}$  is close to the  $x_p$  intersection of  $\alpha_{\text{AB}} = 1$  with the AE edge when  $F_E/F$  decreases. Then, the content of acetone in  $\text{SN}_{\text{ext,A}'}$  increases, and so does the efficiency indicator  $E_{\text{ext}}$ . (3) The efficiency indicator decreases at fixed  $F_E/F$  following the decrease of  $R_1$ . The reason is that as the reflux ratio decreases, the unstable separatrix moves toward the distillate composition and narrows the feasible region (see Figure 2). Therefore,  $E_{\text{ext}}$  is likely to decrease following the meaning of  $E_{\text{ext}}$ . From another view, as the reflux ratio decreases for a fixed distillate, the liquid flow rate from column top to the main feed tray decrease, leading to the acetone content on the main feed tray increasing relatively, so  $E_{\text{ext}}$  decreases following its definition.

From Figure 6, we know that (1) there are only a few points belonging to the Pareto front in the region of reflux ratio  $R_1$  lower than 4 and entrainer flow  $F_E$  higher than 700 kmol/h. At a relatively high entrainer flow rate, the separating cost in the regeneration column increases. Then, TAC increases compared

with the design at a more suitable entrainer flow rate, leading to fewer designs in this region to be ranked in the Pareto front. (2) At low  $F_E$  (400–500 kmol/h) and reflux ratio (2.4–2.8), no designs are ranked. For these values, the specification of product purities is difficult to achieve for finite tray numbers. (3) Finally, for the value  $P_1 = 0.6$  atm that we chose, an economically feasible value range of the entrainer flow rate is (450–650 kmol/h), namely, (0.83–1.2) for  $F_E/F$ .

**3.3. Analysis of Ternary Extractive Profiles Map for Selected Designs.** To further understand the effect of the efficiency indicator  $E_{\text{ext}}$  on the process, we extract from Figure 4 the relation map of  $E_{\text{ext}}$  and TAC and analyze some designs from the Pareto front, namely G1–G6, as shown in Figure 7.

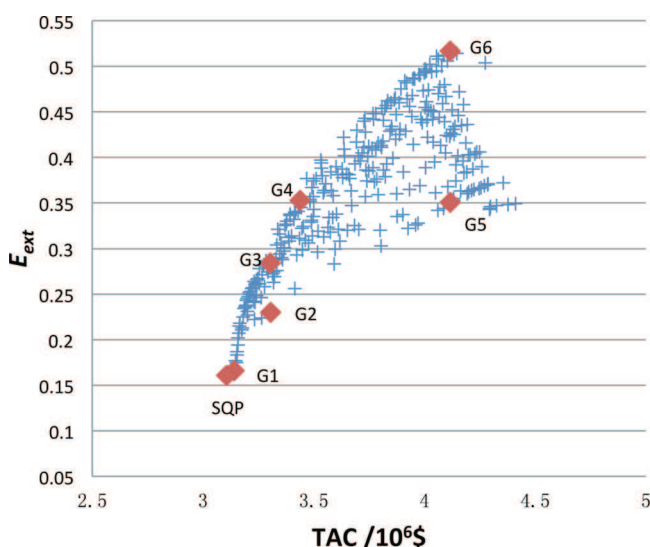


**Figure 7.** Relation map of  $E_{\text{ext}}$  and TAC for some designs from Pareto front.

G1, G3, G4, and G6 are chosen on the upper border of the Pareto front. G2 has a TAC close to that of G3 but exhibits a lower efficiency indicator  $E_{\text{ext}}$ . G5 has the same  $E_{\text{ext}}$  as G4 but a much higher TAC. Table 1 shows the design variables of G1–G6 and Table S1 (in the Supporting Information) provides the sizing parameters and cost data.

We question the reasons for the occurrence of the upper border of the Pareto front, and we display the extractive section profile map of G3 at 0.6 and 1 atm and the simulating composition profile in Figure 8.

Following the physical meaning of  $E_{\text{ext}}$ , we can infer that the efficiency indicator will be the highest at low  $F_E/F$  ratio when the stable node of the extractive section is more close to  $x_p$ , and when the extractive section profile nears the unstable extractive separatrix. The second condition is nearly achieved for G3 design, as shown in Figure 8.

The use of the approximate differential extractive profile map derived from mass balance and assuming an infinite number of trays is relevant as Figure 3 shows that the approximate profile shape agrees with the simulated one, which is calculated with rigorous MESH equations at given tray number for each section. We observe that at point G3, the first condition for maximizing the efficiency indicator is not achieved. Indeed, the process is feasible as the stable node of the extractive section  $\text{SN}_{\text{ext,A}'}$  is close to the AE side but as the  $F_E/F$  (0.98) is bigger than the minimum value 0.19 and the reflux ratio 3.00 is bigger than the minimum value 2.00,  $\text{SN}_{\text{ext,A}'}$  lies far from  $x_p$ . Figure 8

**Table 1. Design Parameters for G1–G6 Belonging to the Pareto Front,  $P_1 = 0.6 \text{ atm}$ ,  $P_2 = 1 \text{ atm}$**

	G1	G2	G3	G4	G5	G6
Extractive Column						
$N_1$	65	65	65	61	64	65
$F_{AB}$ (kmol/h)	540.0	540.0	540.0	540.0	540.0	540.0
$W_2$ (kmol/h)	545.3	616.3	525.7	431.4	864.8	400.4
$E_{\text{makeup}}$ (kmol/h)	1.7	1.6	1.9	1.3	1.5	1.3
$F_E$ (kmol/h)	547.0	617.9	527.6	432.7	866.3	401.7
$N_{F,E}$	34	37	33	26	31	25
$N_{F,AB}$	53	52	54	49	43	55
$D_1$ (kmol/h)	271.3	271.3	271.3	271.3	271.3	271.3
$R_1$	2.66	2.98	3.00	3.44	4.64	4.98
$Q_C$ (MW)	8.38	9.10	9.15	10.17	12.91	13.92
$Q_R$ (MW)	8.71	9.49	9.47	10.41	13.49	13.69
Regeneration Column						
$N_2$	35	35	35	35	35	35
$D_2$ (kmol/h)	270.4	270.3	270.6	270.0	270.2	270.0
$N_{FR}$	26	24	28	27	26	25
$R_2$	1.02	1.05	1.05	1.04	1.20	1.03
$Q_C$ (MW)	5.32	5.41	5.43	5.39	5.82	5.35
$Q_R$ (MW)	5.70	5.81	5.80	5.72	6.34	5.66
OF (kJ/kmol)	28657.5	30429.8	30368.2	32111.7	39431.6	38964.8
TAC ( $\times 10^6$ \$)	3.140	3.305	3.304	3.438	4.115	4.117
$E_{\text{ext}}$ ( $\times 10^{-3}$ )	166	230	284	353	351	517
$e_{\text{ext}}$ ( $\times 10^{-3}$ )	8.3	14.4	12.9	14.7	27.0	16.7

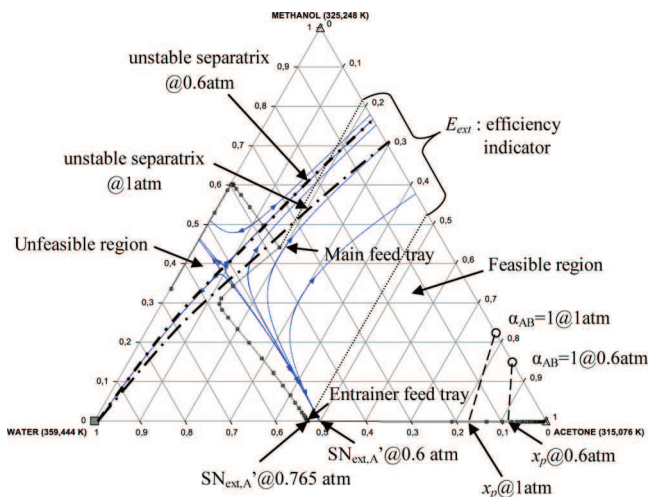


**Figure 8.** Extractive section profile map for acetone–methanol–water, case G3.

also shows that as the extractive unstable separatrix moves inside the diagram, giving rise to a shrinking unfeasible composition region when the reflux ratio decreases, the composition's location of main feed stage should be at the lower side of the unstable separatrix; otherwise the process will be unfeasible as the extractive profiles no longer reach  $SN_{\text{ext},A}'$  and acetone is no longer the distillate. In addition, when the reflux ratio increases, the separatrix is closer to the BE side, to larger feasible region, leading to a higher value of the efficiency indicator. This point was observed in Figure 5 and agrees with the statement about the feasibility of extractive distillation.<sup>11,14</sup> However, increasing  $R_1$  is not always a good way to obtain a higher  $E_{\text{ext}}$  as the energy cost and TAC will increase. In our previous work,<sup>28</sup> we found that a better way to improve the design is to change  $F_E/F$  and the suitable feed location to increase the average relative volatility.

In Table 1, the G1 design exhibits the lowest TAC and represents our so-called optimal design from the NSGA optimization. Comparing the designs of G2 and G3 points with the same total number of trays and nearly the same reflux ratio, OF and TAC, we notice that G3 shows an  $E_{\text{ext}}$  higher than that of G2 because of a lower  $F_E/F$ , but G2 has a higher  $e_{\text{ext}}$  than G3 because the G2 extractive section is shorter than G3 (16 trays versus 22). We may infer that for the same TAC and OF, lowering the entrainer feed flow rate (G3) can be compensated by a higher efficiency per tray (G2).

Comparing G4 and G5, (1) G5 TAC is much higher than G4's because the much larger  $F_E/F$  and a large reflux ratio for G5 induce larger reboiler and condenser duties and raise the OF and TAC. This indicates that a decrease of the entrainer flow rate and  $R_1$  due to more suitable feed locations  $N_{F,AB}$  and  $N_{F,E}$  in the design of G4 greatly reduces the OF and TAC. This point proves the importance of increasing the tray number in the extractive section to 24 trays for the design of G4 and 13 trays for the design of G5. As discussed in our earlier works<sup>28</sup> and Lelkes et al.,<sup>40</sup> the extractive section should have enough trays so that the composition at the entrainer feed tray lies near the stable node of the extractive section  $SN_{\text{ext},A}'$  that should be as close as possible to the product–entrainer edge. This point is also in agreement with the sensitivity analysis over the tray number performed by Lang for the same separating system.<sup>41</sup> (2) G5 design shows that a high extractive efficiency indicator per tray  $e_{\text{ext}}$  does not always mean low OF and TAC. Compared to G4, the increase of  $e_{\text{ext}}$  in G5 by decreasing the tray number in the extractive section requires  $F_E/F$  and  $R_1$  to be increased in order to get the same  $E_{\text{ext}}$  for both G4 and G5. This leads to the increase of TAC due to the increase of the energy cost in extractive column and the separation in entrainer recovery column.

When the designs of G3 and G4 are compared, both on the upper frontier of the Pareto front, the higher  $E_{\text{ext}}$  for G4 is due to the decrease of  $F_E$  that moves  $SN_{\text{ext},A}'$  closer to  $x_p$  and to the

increase of  $R_1$  that approaches the unstable separatrix closer to the BE edge.

Finally, G6 and G1 display the best and the worst value of the efficiency indicator. G6's very high TAC shows that maximizing the total efficiency, by getting the main feed tray composition near the unstable extractive separatrix and by looking for the lowest entrainer flow rate, does not lead to the lowest OF and TAC design. On the contrary, the best design G1 shows the lowest  $E_{\text{ext}}$  but it is still larger than the one for Luyben's design,<sup>19</sup>  $E_{\text{ext}} = 55 \times 10^{-3}$ , and close to that of Knapp and Doherty's design,<sup>42</sup>  $E_{\text{ext}} = 160 \times 10^{-3}$ , discussed in our previous work.<sup>28</sup>

Figure 9 displays the extractive section profile map and the simulation composition profile for G1.

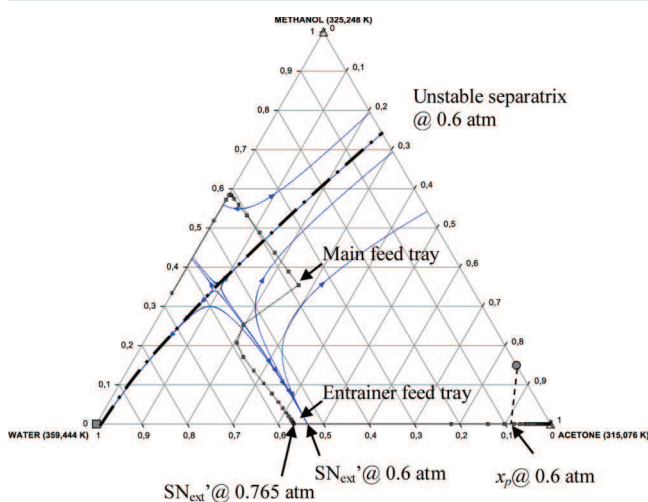


Figure 9. Extractive section profile map for acetone–methanol–water, case G1.

The beginning point of the extractive section (at main feed tray) in the design of G1 (see Figure 9) is not as close to the unstable separatrix as would have been expected from the design of G3 (see Figure 8), and  $E_{\text{ext}}$  is consequently lower. The reasonable explanation is that during the optimization procedure of NSGA with maximizing  $E_{\text{ext}}$ , the reflux ratio ( $R_1$ ) is a dominant variable to reduce OF and TAC. When  $E_{\text{ext}}$  is closer to its optimal value  $E_{\text{ext,opt}}$  the effect of  $R_1$  becomes weak, and meanwhile the effect of other variables (entrainer flow rate, entrainer and main feed locations) become more obvious, leading to a design with lower TAC and the beginning point away from the unstable separatrix. This phenomenon proves that finding an optimal design cannot rely only upon the sole maximization of  $E_{\text{ext}}$ , but that further optimization is necessary for a given  $R_1$  and  $F_E$ .

This answers our initial question and tempers our optimism displayed in our previous work: we cannot use the efficiency indicator alone to optimize the extractive distillation process for the 1.0-1a class, and there likely exists an optimal  $E_{\text{ext,opt}}$  near G1's values that we now verify.

**3.4. Further Improvement of GA's Optimal Design.** As stated earlier, the Pareto front displaying the results is merely an approximation obtained by the stochastic optimization; nature cannot guarantee that each point is a true optimum, expected to border the Pareto front. Also, they are obtained through the optimization of the four objective functions, but in practice the design with the lowest TAC is the most favorable

one. So we select the design of G1 which has the lowest TAC as initial design to run a further optimization in order to appreciate the ability of the NSGA to find an optimal solution. The results are shown in Table 2, namely, case SQP. In

Table 2. Final Design Results for Acetone–Methanol–Water of Case 3opt', Case G1, and Case SQP

	case 3opt'	case G1	case SQP
Extractive Column			
$N_1$	57	65	65
$F_{AB}$ (kmol/h)	540	540.0	540.0
$W_2$ (kmol/h)	636.1	545.3	557.9
$E_{\text{makeup}}$ (kmol/h)	2.1	1.7	2.1
$F_E$ (kmol/h)	638.2	547.0	560.0
$N_{F,E}$	32	34	34
$N_{F,AB}$	48	53	55
$D_1$ (kmol/h)	271.0	271.3	271.1
$R_1$	2.74	2.66	2.59
$Q_C$ (MW)	8.55	8.38	8.21
$Q_R$ (MW)	8.93	8.71	8.56
Regeneration Column			
$N_2$	35	35	35
$D_2$ (kmol/h)	271.1	270.4	271.0
$N_{FR}$	19	26	25
$R_2$	1.18	1.02	1.00
$Q_C$ (MW)	5.78	5.32	5.30
$Q_R$ (MW)	6.21	5.70	5.68
OF (kJ/kmol)	30119.8	28657.5	28326.3
TAC ( $\times 10^6$ \$)	3.153	3.140	3.107
$E_{\text{ext}}$ ( $\times 10^{-3}$ )	153	166	161
$e_{\text{ext}}$ ( $\times 10^{-3}$ )	9.0	8.3	7.3

addition, in order to compare fairly with our previous design<sup>28</sup> ( $N_1 = 57$ ,  $N_2 = 26$ ), namely, case 3opt in which a 100% tray efficiency was assumed and the pressure drop per tray was neglected, we now optimize it as case 3opt' under 85% tray efficiency and a 0.005 atm pressure drop per tray. The results are shown in Table 2, while Supporting Information Table S2 shows the sizing figures and cost data.

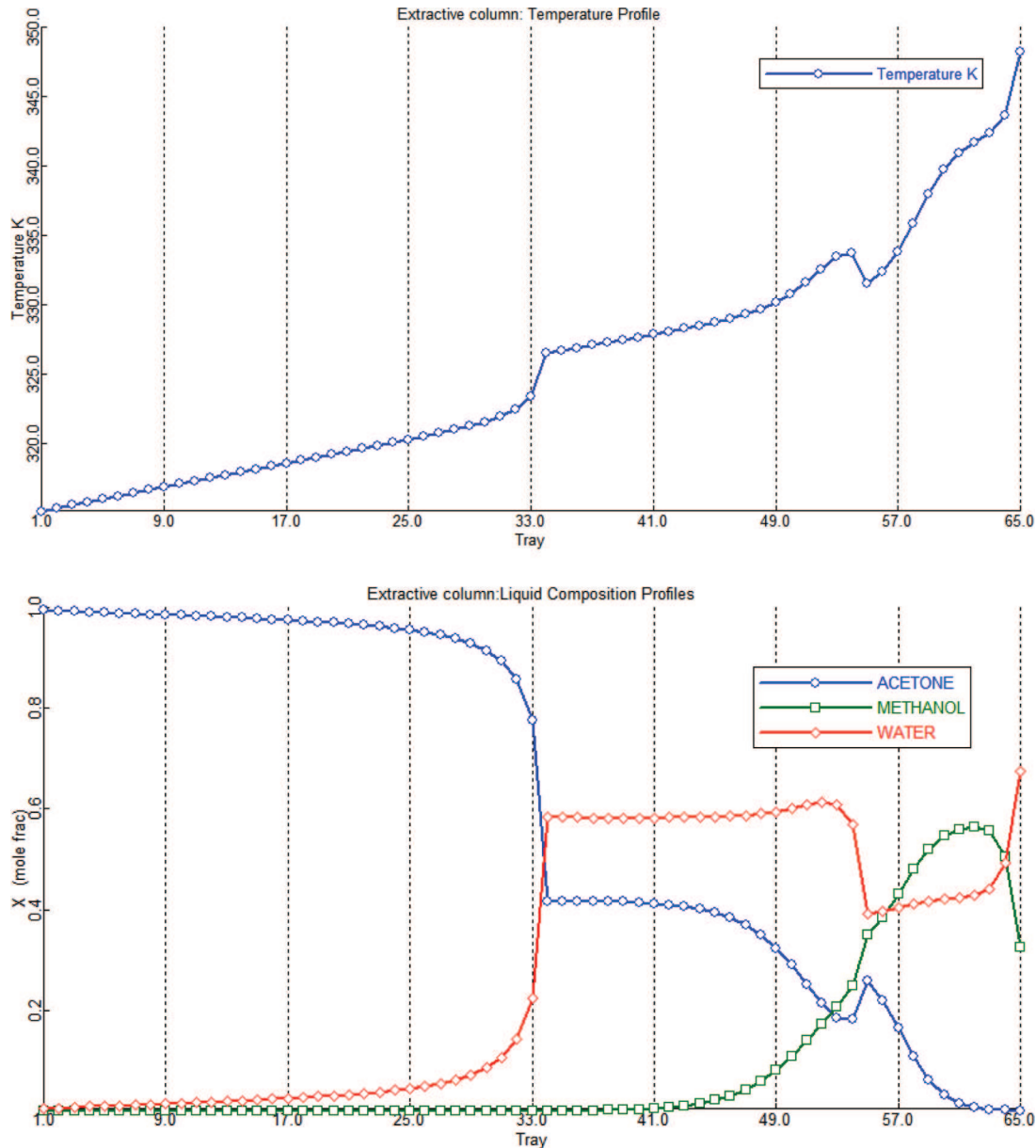
The single objective function is energy cost OF and is based on the same column tray number ( $N_1 = 57$ ,  $N_2 = 26$ ) for case 3opt' and ( $N_1 = 65$ ,  $N_2 = 35$ ) for case SQP. The other eight variables are optimized through minimizing OF by using the two-step optimization procedure stated in previous work.<sup>28</sup> TAC and two efficiency indicators are calculated afterward. The design and operating variables are shown in Table 2, referring to the flow sheet notations in Figure 1. Table 3 displays the product purity and recovery values.

Table 3 shows that case 3opt', G1, and SQP optimized in closed-loop flow sheet achieve the product purities for both distillates. We also notice that the water content in recycled entrainer is very high for all cases but lower than 99.99% in case G1 obtained with the NSGA optimization. In our previous work,<sup>28</sup> on the basis of a SQP optimization with an open loop flow sheet assuming a pure entrainer feed to the extractive column, we had to run an additional closed-loop simulation to overcome the effects of the impurities in recycled entrainer on the product purity. This is no longer necessary with the NSGA method optimizing directly the closed-loop flow sheet.

With the same number of trays as Luyben and Knapp and Doherty's design but with stricter product purity constraints, Table 2 shows that case 3opt in You's work<sup>28</sup> represented a

**Table 3. Product Purities and Recoveries for Case 3opt', Case G1, and SQP Designs**

mole fraction		$D_1$	$D_2$	$W_2 = \text{water}$	$W_1 = F_2$	recovery
case 3opt'	acetone	0.99502	0.00129	$8.10 \times 10^{-11}$	0.00039	99.87%
	methanol	0.00055	0.99540	0.00009	0.29753	99.95
	water	0.00443	0.00331	0.99991	0.70208	
case G1	acetone	0.99502	0.00019	$1.43 \times 10^{-12}$	$6.22 \times 10^{-5}$	99.98%
	methanol	0.00053	0.99799	0.000143	0.33089	99.95%
	water	0.00445	0.00182	0.999857	0.66905	
case SQP	acetone	0.99505	0.00090	$9.58 \times 10^{-13}$	0.00029	99.91%
	methanol	0.00023	0.99608	$4.36 \times 10^{-5}$	0.32568	99.98%
	water	0.00472	0.00302	0.999956	0.67403	



**Figure 10.** Temperature and composition profiles of extractive column for the extractive distillation of acetone–methanol with water, case SQP.

great improvement over Luyben’s design with a double-digit saving in OF and TAC and reached OF = 28318.5 kJ/kmol and TAC =  $2.918 \times 10^6$  \$ per year (see ref 28). By taking into account the tray efficiency and the pressure drop, case 3opt’ OF and TAC increase now to OF = 30119.8 kJ/kmol and TAC =  $3.153 \times 10^6$  \$ per year, mostly because of the decrease of the

tray efficiency. The pressure drop slightly affects the relative volatility, which decreases when the pressure increases.<sup>28</sup> Therefore, the TAC and OF are slightly larger.

From Table 2, we also know that (1) the G1 design reduces OF by 4.8% over case 3opt’. A suitable increase of tray number proposed by the NSGA optimization in the columns allows a

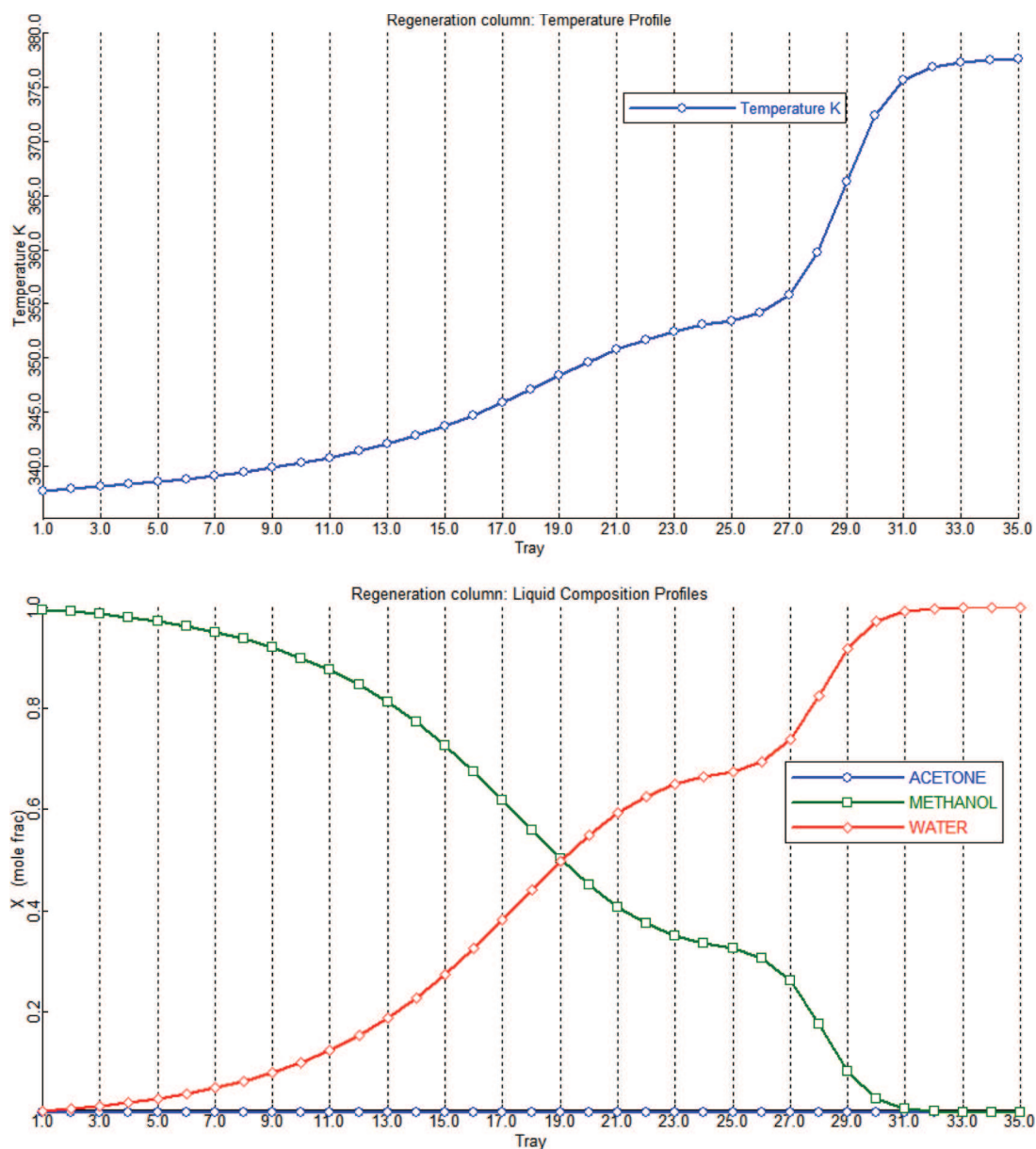


**Figure 11.** Temperature and composition profiles of entrainer regeneration column for the extractive distillation of acetone–methanol with water, case SQP.

lower entrainer flow rate to be used and decreases the energy cost in both columns. (2) The G1 design from NSGA with four objective functions is marginally improved through the sensitivity analysis plus ASPEN built-in SQP method that only minimizes OF. At the design step of the process, the improvement is not significant. (3) The ASPEN built-in SQP method runs faster than NSGA. Also, it can be initialized by the NSGA results. (4) Compared with case G1, two more trays are used in the extractive section of case SQP design, resulting in a small decrease of the reflux ratio in extractive column. (5) For the acetone–methanol equimolar mixture separation with water,  $E_{ext,opt}$  should be at  $0.161 \pm 3\%$  for extractive column operating at 0.6 atm. It is greater than Luyben's figure and similar to Knapp and Doherty's estimate (see ref 28).

The temperature and composition profiles in the two columns of case SQP are shown in Figures 10 and 11. When displayed on a ternary diagram, the case SQP composition

profile looks very similar to the one for G1 displayed in Figure 8.

From Figure 10, there is a temperature decrease in the temperature profile map of the extractive column as the main feed temperature was fixed at 320 K during the optimization the same as previous design.<sup>28</sup> We can also notice in Table 3 that most of the impurity in the distillate ( $D_1$ ) is the high-boiling temperature water because the rectifying section profile reaches  $x_{D_1}$  on the acetone–water mixture side where there is a pinch point at the high acetone content side. Its effect is that more than half of the trays (34 out of 65) are used in rectifying section in extractive column for separating the acetone from water. In addition, the content of methanol in the rectifying section is very low (see Figure 11), which proves that the extractive section pinch point ( $SN_{ext}'$ ) was able to come very close to the AE side.

## 4. CONCLUSION

The optimization of the extractive distillation process including the extractive and entrainer regeneration columns for the separation of acetone–methanol minimum azeotropic mixture with heavy entrainer water was investigated. It was intended to find out whether efficiency indicators describing the ability of the extractive section to discriminate the product between the top and the bottom of that section could be used to optimize the process design because we had found previously that improvement of some designs in the literature leads to an increase in those indicators, not an unexpected result because they describe the main goal of the extractive distillation process. A multiobjective nonsorted genetic algorithm method coded in Excel was used as optimization method, and it was linked with Aspen plus software through programming in VBA. We run the optimization with four objective functions: extractive efficiency indicator  $E_{\text{ext}}$  and  $e_{\text{ext}}$  are maximized while TAC (economic view) and OF (energy cost per unit product) are minimized while 99.5% products purities in the distillates are set as constraints.

Through the analysis of the Pareto front, the effects of the main variables, entrainer-to-feed ratio and reflux ratio, on TAC and efficiency indicator were discussed. They were also analyzed with respect to thermodynamic insights underlying the extractive section composition profile map. The results show that the efficiency indicators cannot be used alone for optimizing the process design, but they help understand designs that are better than others. There is a maximum  $E_{\text{ext}}$  for a given reflux ratio, and there is a minimum  $R_1$  for a given  $E_{\text{ext}}$ . There also exists an optimal efficiency indicator  $E_{\text{ext,opt}}$  which corresponds to the optimal design defined as the one with the lowest TAC, and  $E_{\text{ext,opt}}$  can be used as a criterion for evaluating different designs for the same system. For the acetone–methanol with water system,  $E_{\text{ext,opt}}$  equals  $0.161 \pm 3\%$  at 0.6 atm. Indeed, we have to conclude that although the efficiency indicators cannot be used as an optimization criterion alone, it is worth combining it with usual criteria such as TAC and OF because near its  $E_{\text{ext,opt}}$  value the design is still very sensitive to the entrainer feed flow rate and reflux ratio parameters that have a dominant impact on the OF and TAC. Through the analysis of extractive profile maps, we also explain the reasons why the efficiency indicator increases following the decrease of entrainer flow rate and the increase of reflux ratio.

The ASPEN built-in SQP method is used to further improve the design following the decrease of TAC with the initial values from the NSGA method. A competitive design is found but with only a <1% marginal improvement, showing that NSGA optimization with the four criteria described above is able to find a consistent design for the extractive process concerning the 1.0-1a class mixture.

## ■ ASSOCIATED CONTENT

### 📄 Supporting Information

The Supporting Information is available free of charge on the ACS Publications website at DOI: [10.1021/acs.iecr.5b02015](https://doi.org/10.1021/acs.iecr.5b02015).

Sizing parameters for the columns and cost data of the designs (PDF)

## ■ AUTHOR INFORMATION

### Corresponding Author

\*E-mail: [Vincent.Gerbaud@ensiacet.fr](mailto:Vincent.Gerbaud@ensiacet.fr).

## Notes

The authors declare no competing financial interest.

## ■ ACKNOWLEDGMENTS

X.Y. thanks the Chinese Scientific Council for its support of this work.

## ■ REFERENCES

- (1) Doherty, M. F.; Knapp, J. P. *Distillation, Azeotropic, and Extractive*. In *Kirk-Othmer Encyclopedia of Chemical Technology*; Wiley: New York, 1993.
- (2) Luyben, W. L. *Distillation Design and Control Using Aspen Simulation*. John Wiley & Sons, Inc: New York, 2006.
- (3) Hilmen, E. K. *Separation of Azeotropic Mixtures: Tools for Analysis and Studies on Batch Distillation Operation*. Ph.D. Thesis, Norwegian University of Science and Technology, Trondheim, Norway, 2000.
- (4) Gerbaud, V.; Rodriguez-Donis, I. Extractive distillation. In *Distillation Book*; Gorak, A., Olujic, Z., Eds.; Elsevier: Amsterdam, 2014; Vol. 2, Chapter 6, pp 201–247.
- (5) Lelkes, Z.; Láng, P.; Benadda, B.; Otterbein, M.; Moszkowicz, P. Batch Extractive Distillation: the Process and the Operational Policies. *Chem. Eng. Sci.* **1998**, *53*, 1331.
- (6) Lang, P.; Yatim, H.; Moszkowicz, P.; Otterbein, M. Batch Extractive Distillation Under Constant Reflux Ratio. *Comput. Chem. Eng.* **1994**, *18* (11), 1057.
- (7) Düssel, R.; Stichlmair, J. Separation of Azeotropic Mixtures by Batch Distillation Using an Entrainer. *Comput. Chem. Eng.* **1995**, *19*, 113.
- (8) Doherty, M. F.; Perkins, J. D. On The Dynamics of Distillation Process III. The Topological Structure of Ternary Residue Curve Maps. *Chem. Eng. Sci.* **1979**, *34*, 1401.
- (9) Widagdo, S.; Seider, W. D. Journal Review Azeotropic Distillation. *AIChE J.* **1996**, *42*, 96–130.
- (10) Ravagnani, M.; Reis, M. H. M.; Filho, R. M.; Wolf-Maciel, M. R. Anhydrous Ethanol Production by Extractive Distillation: A Solvent Case Study. *Process Saf. Environ. Prot.* **2010**, *88* (1), 67.
- (11) Rodriguez-Donis, I.; Gerbaud, V.; Joulia, X. Thermodynamic Insights on the Feasibility of Homogeneous Batch Extractive Distillation. 1. Azeotropic Mixtures with Heavy Entrainer. *Ind. Eng. Chem. Res.* **2009**, *48* (7), 3544.
- (12) Andersen, H. W.; Laroche, L.; Morari, M. Dynamics of Homogeneous Azeotropic Distillation Columns. *Ind. Eng. Chem. Res.* **1991**, *30* (8), 1846.
- (13) Laroche, L.; Bekiaris, N.; Andersen, H. W.; Morari, M. The Curious Behavior of Homogeneous Azeotropic Distillation – Implications for Entrainer Selection. *AIChE J.* **1992**, *38*, 1309.
- (14) Shen, W.; Benyounes, H.; Gerbaud, V. Extension of Thermodynamic Insights on Batch Extractive Distillation to Continuous Operation. 1. Azeotropic Mixtures with a Heavy Entrainer. *Ind. Eng. Chem. Res.* **2013**, *52* (12), 4606.
- (15) Bauer, M. H.; Stichlmair, J. Synthesis and Optimization of Distillation Sequences for the Separation of Azeotropic Mixtures. *Comput. Chem. Eng.* **1995**, *19*, 15.
- (16) Wahnschafft, O. M.; Westerberg, A. W. The Product Composition Regions of Azeotropic Distillation Columns. 2. Separability in Two-feed Columns and Entrainer Selection. *Ind. Eng. Chem. Res.* **1993**, *32* (6), 1108.
- (17) Brüggemann, S.; Marquardt, W. Shortcut Methods for Nonideal Multicomponent Distillation: 3. Extractive Distillation Columns. *AIChE J.* **2004**, *50* (6), 1129.
- (18) Vazquez-Ojeda, M.; Segovia-Hernandez, J. G.; Hernandez, S.; Hernandez-Aguirre, A.; Kiss, A. A. Design and Optimization of an Ethanol Dehydration Process Using Stochastic Methods. *Sep. Purif. Technol.* **2013**, *105*, 90.
- (19) Luyben, W. L. Comparison of Extractive Distillation and Pressure-swing Distillation for Acetone – Methanol Separation. *Ind. Eng. Chem. Res.* **2008**, *47*, 2696.

- (20) Gil, I. D.; Botia, D. C.; Ortiz, P.; Sánchez, O. F. Extractive Distillation of Acetone/Methanol Mixture Using Water as Entrainer. *Ind. Eng. Chem. Res.* **2009**, *48*, 4858.
- (21) Wang, Q.; Yu, B.; Xu, C. Design and Control of Distillation System for Methylal/Methanol Separation. Part 1: Extractive Distillation Using DMF as an Entrainer. *Ind. Eng. Chem. Res.* **2012**, *51* (3), 1281.
- (22) de Figueiredo, M. F.; Guedes, B. P.; De Araujo, J. M.; Vasconcelos, L. G. S.; Brito, R. P. Optimal Design of Extractive Distillation Columns—a Systematic Procedure Using a Process Simulator. *Chem. Eng. Res. Des.* **2011**, *89*, 341.
- (23) Kiss, A. A.; Suszwalak, D. J. Enhanced Bioethanol Dehydration by Extractive and Azeotropic Distillation in Dividing-wall Columns. *Sep. Purif. Technol.* **2012**, *86*, 70.
- (24) Kossack, S.; Kraemer, K.; Gani, R.; Marquardt, W. A Systematic Synthesis Framework for Extractive Distillation Processes. *Chem. Eng. Res. Des.* **2008**, *86*, 781.
- (25) García-Herreros, P.; Gómez, J. M.; Gil, I. D.; Rodriguez, G. Optimization of the Design and Operation of an Extractive Distillation System for the Production of Fuel Grade Ethanol Using Glycerol as Entrainer. *Ind. Eng. Chem. Res.* **2011**, *50*, 3977.
- (26) Gutiérrez-Antonio, C.; Briones-Ramírez, A.; Jiménez-Gutiérrez, A. Optimization of Petlyuk Sequences Using a Multi Objective Genetic Algorithm with Constraints. *Comput. Chem. Eng.* **2011**, *35* (2), 236.
- (27) Xu, W.; Diwekar, U. M. Improved Genetic Algorithms for Deterministic Optimization and Optimization Under Uncertainty. Part II. Solvent Selection Under Uncertainty. *Ind. Eng. Chem. Res.* **2005**, *44*, 7138.
- (28) You, X.; Rodriguez-Donis, I.; Gerbaud, V. Improved Design and Efficiency of the Extractive Distillation Process for Acetone-Methanol with Water. *Ind. Eng. Chem. Res.* **2015**, *54* (1), 491.
- (29) Frits, E. R.; Lelkes, Z.; Fonyo, Z.; Rev, E.; Markot, M. C.; Csendes, T. Finding Limiting Flows of Batch Extractive Distillation with Interval Arithmetics. *AIChE J.* **2006**, *52* (9), 3100.
- (30) Petlyuk, F.; Danilov, R.; Burger, J. A Novel Method for the Search and Identification of Feasible Splits of Extractive Distillations in Ternary Mixtures. *Chem. Eng. Res. Des.* **2015**, *99*, 132.
- (31) Knapp, J. P.; Doherty, M. F. Minimum Entrainer Flow for Extractive Distillation: A Bifurcation Theoretic Approach. *AIChE J.* **1994**, *40*, 243.
- (32) Kiva, V. N.; Hilmen, E. K.; Skogestad, S. Azeotropic Phase Equilibrium Diagrams: A Survey. *Chem. Eng. Sci.* **2003**, *58*, 1903.
- (33) Hilmen, E. K.; Kiva, V. N.; Skogestad, S. Topology of Ternary VLE Diagrams: Elementary Cells. *AIChE J.* **2002**, *48* (4), 752.
- (34) Gomez, A.; Pibouleau, L.; Azzaro-Pantel, C.; Domenech, S.; Latge, C.; Haubensack, D. Multiobjective Genetic Algorithm Strategies for Electricity Production from Generation IV Nuclear Technology. *Energy Convers. Manage.* **2010**, *51* (4), 859.
- (35) You, X.; Rodriguez-Donis, I.; Gerbaud, V. Extractive Distillation Process Optimisation of the 1.0-1a Class System, Acetone-Methanol with Water. In *24th European Symposium on Computer Aided Process Engineering*; Klemes, J. J., Varbanov, S. V., Liew, P. Y., Eds.; Elsevier: Amsterdam, 2014.
- (36) Douglas, J. M. *Conceptual Design of Chemical Processes*; McGraw-Hill: New York, 1988.
- (37) Marshall & Swift. Average M & S index for year 2011. *Chem. Eng.* **2012**, *119*, 84.
- (38) Botia, D. C.; Riveros, D. C.; Ortiz, P.; Gil, I. D.; Sanchez, O. F. Vapor–Liquid Equilibrium in Extractive Distillation of the Acetone/Methanol System Using Water as Entrainer and Pressure Reduction. *Ind. Eng. Chem. Res.* **2010**, *49*, 6176.
- (39) De Figueiredo, M. F.; Brito, K. D.; Ramos, W. B.; Vasconcelos, L. G. S.; Brito, R. P. Effect of Solvent Content on the Separation and the Energy Consumption of Extractive Distillation Columns. *Chem. Eng. Commun.* **2015**, *202* (9), 1191.
- (40) Lelkes, Z.; Lang, P.; Benadda, B.; Moszkowicz, P. Feasibility of Extractive Distillation in a Batch Rectifier. *AIChE J.* **1998**, *44*, 810.
- (41) Lang, P. Computation of Multicomponent, Multistage Separation Processes. In *Studies in Computer-Aided Modelling, Design and Operation: Unit Operations*; Pallai, I., Fonyo, Z., Eds.; Elsevier: Budapest, 1992; Chapter 7, pp 256.
- (42) Knapp, J. P.; Doherty, M. F. Thermal Integration of Homogeneous Azeotropic Distillation Sequences. *AIChE J.* **1990**, *36*, 969.